



available at www.sciencedirect.com



journal homepage: www.elsevier.com/locate/jhydrol



Rating curves and estimation of average water depth at the upper Negro River based on satellite altimeter data and modeled discharges

J.G. Leon ^{a,*}, S. Calmant ^b, F. Seyler ^a, M.-P. Bonnet ^a, M. Cauhopé ^a,
F. Frappart ^{a,b}, N. Filizola ^c, P. Fraizy ^a

^a *Laboratoire des Mécanismes et Transferts en Géologie, (IRD, CNRS, UPS), 14 Av. Edouard Belin, 31400 Toulouse, France*

^b *Laboratoire d'Etudes en Géophysique et Océanographie Spatiales, (IRD, CNRS, UPS), 14 Av. Edouard Belin, 31400 Toulouse, France*

^c *University of the Amazonas State, Brazil*

Received 20 October 2005; received in revised form 23 December 2005; accepted 23 December 2005

KEYWORDS

Rating-curve;
Effective zero flow;
Radar altimetry;
Manning coefficient;
Negro River;
Amazon Basin

Summary The objective of this study is to derive the stage–discharge relationship for 21 “virtual gauge stations” located at the upper Negro River (Amazon Basin, Brazil). A virtual station can be defined as any crossing of water body surface (i.e., large rivers) by radar altimeter satellite tracks. Rating curve parameters are estimated by fitting with a power law the temporal series of water surface altitude derived from satellite measurements and the discharge. Discharges are calculated using ProGUM, a flow routing model based on the Muskingum–Cunge (M–C) approach considering a diffusion-cum-dynamic wave propagation [Leon, J.G., Bonnet, M.P., Cauhopé, M., Calmant, S., Seyler, F., submitted for publication. Distributed water flow estimates of the upper Negro River using a Muskingum–Cunge routing model based on altimetric spatial data. *J. Hydrol.*]. Among these parameters is the height of effective zero flow. Measured from the WGS84 ellipsoid used as reference, it is shown that the height of effective zero flow is a good proxy of the mean water depth from which bottom slope of the reaches can be computed and Manning roughness coefficients can be evaluated. Mean absolute difference lower than 1.1 m between estimated equivalent water depth and measured water depth indicates the good reliability of the method employed. We computed the free surface water slope from ENVISAT altimetry data for dry and rainy seasons. These profiles are in good agreement with the bottom profile derived from the aforementioned water depths. Also, the corresponding Manning coefficients are consistent with the admitted ranges for natural channels with important flows (superficial width >30.5 m [Chow, V.T., 1959. *Open Channel Hydraulics*. McGraw-Hill, New York]) and irregular section.
© 2006 Elsevier B.V. All rights reserved.

* Corresponding author. Tel.: +33 5 61 33 26 62.
E-mail address: leon@lmtg.obs-mip.fr (J.G. Leon).

Introduction

Monitoring of the temporal variations of the river water levels is classically made using in situ recordings. Level variations can be expressed in terms of discharges using calibrated relationships referred to as rating curves. However, most large river basins in the world, e.g., the Amazon Basin in South America, cover areas of difficult access. This is a major hindrance to the installation of operational networks of hydrological in situ stations. Radar altimetry is an interesting alternative to recording the periodic measurements of water level variations in the continental environment even in these remote places. The ability of radar altimeters to monitor continental water surfaces and measure their stage elevation has been demonstrated over inland waters (Birkett, 1995; Cazenave et al., 1997). However, due to the size of the footprint, it is mainly applicable to large water bodies, particularly the survey of level fluctuations in lakes, large rivers or flood plains.

Leon et al. (submitted for publication) have proposed a bibliographic review of the recent use of radar altimetry over continental water bodies (continental seas, then lakes and large rivers). Normally, land water investigators have to deal with dataset primarily collected and processed for other scientific targets, namely heights collected for either oceans (T/P, Jason, GFO, part of ERS 1 and 2 and ENVISAT) or ice caps (ERS 1 and 2, ENVISAT, ICESat). Thus, T/P measurements have been found to present an overall uncertainty over continental waters of a couple of decimeters (Birkett et al., 2002). Nevertheless, a better accuracy (of the order of a decimeter) have been found on the same continental water bodies with the ICE1 retracked ENVISAT data, which are used in this study (Frappart et al., 2006).

In hydrology, data obtained from satellites and other remote sources support broad and potentially frequent global coverage of river discharge estimates (Barrett, 1998). Thus, a method based on remotely sensed data to estimate river discharge would provide a means to maintain or even increase the global streamflow monitoring network. This could prove cost-effective in the long term to obtain the required river discharge data on a global scale. For example, Jasinski et al. (2001) used river stage data from TOPEX/Poseidon satellite altimetry data to assess discharge ratings in several locations of the Amazon basin by comparing altimetry data with stage and discharge measured at the existing gaging stations. The accuracy of ratings varied depending on distance between altimetry observation and ground-measured discharge, and on topography and the river width. This study demonstrated the feasibility of satellite altimetry for getting remote river stage information. However, ground-based discharge data were required to develop the rating, and the derived ratings could not be extrapolated to other rivers or reaches of the Amazon.

On the other hand, in the case of a large river for example, with a measured discharge record available, even some distance away, this information can be used as an indication of the local hydraulic conditions associated with a particular discharge. The simplest way to do this would be to compile the relationships between local stages and remote discharges. This approach would be adequate under reasonably steady flow conditions but quite inaccurate for highly variable flows

with short duration events, as in many South African rivers, where the distance between the measured discharge and the required stage is large (Birkhead and James, 1998).

Under these conditions the relationship between local stage and local discharge is sought. Establishing this relationship requires accounting for the lag and attenuation of discharge between local and remote sites. Discharges at local and remote sites can be related using a variety of flood routing procedures ranging in simplicity from Muskingum or M–C models to solution of the full dynamic flow (Saint–Venant) equations. Expressing the local stage–discharge relationship as a simple mathematical function, from remote discharge estimated by flow routing model and local stage from radar altimeter, enables the local flow conditions to be expressed in terms of stage or vice versa.

The M–C method has been used in different studies (Boroughs and Zagana, 2002; Johnson and Miller, 1997; Merkel, 1999; Richey et al., 1989) for discharge estimation. Leon et al. (submitted for publication) have estimated the outflows at some virtual gauge stations (places where footprint of radar satellites cross-cut the river channel or the flood plain) for some watersheds of the upper Negro River main channel and tributaries using ProGUM, a M–C flow routing model with diffusion-cum-dynamic wave propagation assumption; in situ discharges and radar altimetry data. In this study, the calibration phase led to differences less than 4% between measured and estimated outflows and validation has given errors less than 10%.

In this paper, it is shown that mean reach depths can be derived from the parameters of the power law establishing the rating curve between water stages from satellite altimetry and discharges estimated by flow routing. First, in situ and altimetry available data are discussed. Then, the method already reported in Leon et al. (submitted for publication) for predicting remote discharges at virtual stations based on the M–C flow routing model approach and in situ data using PROGUM is reviewed. Also discussed is the method to select and retrieve altimeter water levels from TOPEX/Poseidon and ENVISAT over the upper Negro River in the Brazilian Amazon basin. Finally, the method developed in this study to establish stage–discharge relationships between satellite-derived water level and river discharge at 21 virtual stations in the Upper Negro Basin is presented. Expressed as a power law, these relationships allow us to estimate the base of the equivalent wet section depth of the river, referred to here as the average water depth. The resulting slope has been compared with the water free surface slope derived from ENVISAT measurements. The same method has been applied to in situ water level measurements. The resulting average water depth at virtual and in situ stations is compared with mean depth obtained from acoustic Doppler current profiler (ADCP) measurements conducted in May 2005.

Material and methods

The Negro River system

Because of his huge discharges, Amazon River is the most important continental water source in the world. Draining an area of 6.7 million km² the Amazon Basin contributes about 15–20% of all liquid fresh water transported to the

Table 1 Principal characteristics of Negro River

Negro Basin	
Area	715,000 km ²
Mean annual temperature	26 °C
Annual rainfall	3000–4000 mm
Soil moisture regime	Udic to Perudic
Rainfall peak period	April–June
Discharge Ranges	4200–50,000 m ³ /s

Soil Survey Staff (1975, 1990), Dubroeuq and Volkoff (1998) and Guyot (1993).

oceans (Richey et al., 1989; Coe et al., 2002). Negro River, Solimoes River and Madeira River are the three main tributaries of the Amazon.

Negro River Basin extends from 3°14'S to 5°8'N latitude and from 72°57'W to 58°16'W longitude. The basin drains approximately 10% of the Amazon Basin from its source at the confluence of the Guainia River (Colombia border) and Casiquiare River (Venezuela border) to the confluence with Solimoes River, a few kilometres before Manaus (Brasil). Table 1 summarizes the main characteristics of the Negro Basin.

Negro River level and discharge data

In situ gauge station data

For the purpose of this study, the subwatersheds based on in situ gauges are shown in Fig. 1. Four stations are located along the Negro River main stream (Cucui, Sao Felipe, Curicuriari and Serrinha) accounting for a total length of 509 km; two lies in the Uaupes River (Uaracu and Taraqua) representing 387 km. Uaupes River is the main gauged tributary of the upper Negro River. Table 2 summarizes the Negro River main stream features discharges at these six gauged stations and their principal characteristics.

Daily measurements of the river water stage started some time between 1977 and 1982. These records, along with periodical measurements of cross-sectional area, water surface width, flow velocity, bed channel depth are available at the ANA (Brazilian Water National Agency) website (<http://hidroweb.ana.gov.br/>). These measurements have been made by ANA with conventional measurements methods such as reels currentmeter method for discharge. More information acquired during several field campaign from 1995 to now has been found at the HYBAM web site (<http://www.mpl.ird.fr/hybam/campagnes/campagnes.htm>). The discharge measurements retrieved from this site were acquired by ADCP measurements. ADCP profiles are meant

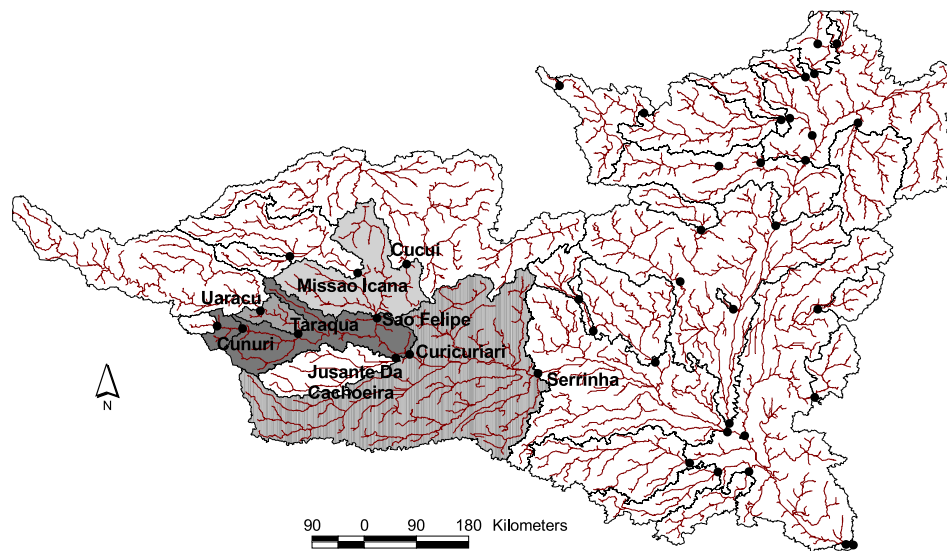


Figure 1 Negro River Basin. The Negro River and the subwatershed delineation. Black points show the position of the hydrological stations in the basin. In grey are the subwatersheds considered in this study.

Table 2 Main characteristics of hydrologic stations studied

Station name	River	Longitude	Latitude	Measurement period	Discharge (m ³ /s)	Drained area (km ²)	Upstream station
Cucui	Negro River	-66.8597	1.2155	1980–2204	400–10,500	70,400	—
Sao Felipe	Negro River	-67.3218	0.3727	1977–2004	1200–15,500	119,200	Cucui
Curicuriari (from Sao Felipe)	Negro River	-66.8115	-0.1921	1977–2004	2500–24,000	132,000	Sao Felipe
Curicuriari (from Taraqua)	Negro River	-66.8115	-0.1921	1977–2004	2500–24,000	132,000	Taraqua
Serrinha	Negro River	-64.8108	-0.4876	1977–2004	5000–30,000	283,000	—
Uaracu	Uaupes River	-69.1388	0.4892	1977–2004	80–6000	38,700	—
Taraqua	Uaupes River	-68.5534	0.1349	1977–2004	250–6500	42,000	Uaracu

to retrieve both discharge and flow velocity in unit cells distributed along verticals every time step (1–3 s in most cases). The computed discharge is the sum of discharge per cell unit and the profile geometry is another possible output of the ADCP software TRANSECT.

Data acquired during a field campaign in May 2005

A field campaign took place in May 2005 and allowed to acquire in situ data, in particular ADCP measurements, in order to assess the quality of the altimeter derived measurements. To perform these measurements on the modelled part of Rio Negro, our team used three light motor boats to follow up the Negro River to Cucui and the Uaupes River to Taraqua, and back to Sao Gabriel da Cachoeira, which lies downstream the confluence Negro–Uaupes in the middle of a succession of rapids and water falls several kilometres long. Downstream of Sao Gabriel, a medium-sized boat has been used to follow down the Rio Negro to Manaus, performing ADCP profiles at the in situ stations and at the locations of each satellite track crossing. Measurements description and locations can be found at <http://www.mpl.ird.fr/hybam/campagnes/campagnes.htm>.

Satellite altimetry data

Satellite altimetry relies on: radar altimetry and orbitography. Radar altimetry measures the distance between satellite and instantaneous water surface. Orbitography provides satellite altitude relative to a reference ellipsoid. The difference between both distances is the instantaneous water level height relative to the reference ellipsoid. Placed into a repeat orbit, the satellite altimeter overflies a given region at regular time intervals, normally called the repeat cycle, and with a ground track footprint that varies depending on satellite characteristics. In this study, two satellite data sources have been selected, i.e., TOPEX/Poseidon and ENVISAT missions.

Corrections applied to these measurements include ionospheric refraction, dry tropospheric refraction, wet tropospheric refraction, solid earth and pole tides (Renelley et al., 2005). Corrections specific to open ocean environments such as ocean tide, ocean tide loading, inverted barometer effect and sea state bias have been disregarded.

TOPEX/Poseidon altimeter data

The NASA/CNES TOPEX/Poseidon (T/P) satellite was launched in August 1992 on a 66° inclined orbit at 1336 km altitude with a 10 days repeat cycle is. Its ground track spacing is 315 km in equatorial regions. The T/P altimeter data were extracted from the Geophysical Data Records (GDR-Ms) available at the Archiving Validation and Interpretation of Satellite Data in Oceanography (AVISO) data center in the French Centre National d'Etudes Spatiales (CNES) (AVISO, 1996). The data collected consisted of range values from radar echoes at 1/10 s and averaged values at 1 s interval, corresponding to an along-track ground spacing of 596 m and 5.96 km, respectively.

On September 2002 T/P moved to a new orbit midway between its original ground tracks. The former T/P ground tracks are now overflowed by Jason-1. Thus, 354 cycles of recorded data are available for the original orbit and approximately 60 cycles of data for the new orbit. In this study, only the 354 cycles of the original orbit have been retained,

corresponding to a period from December 1992 to July 2002. The region studied is overflowed by the tracks 89, 178 and 245. Altimetric measurements were referenced over WGS84 ellipsoid.

ENVISAT altimetry data

The ENVISAT satellite is the continuity of European Space Agency (ESA) ERS-1 and ERS-2 satellites. ENVISAT carries 10 complementary instruments – including a radar altimeter – to observe such parameters as sea surface topography, high-resolution gaseous emissions, orbitography and the precise tracking system Doris.

Launched in March 2002, ENVISAT has a 35-day repeat cycle and provides observations along its entire ground track over the ocean and continental surfaces, from 82.4° North to 82.4° South. The ENVISAT equatorial ground track spacing is about 85 km and its swath width is a few kilometres only. The ENVISAT altimetry data were downloaded from ESA ftp site. Data consist of range values from radar echoes at 1/20 s and averaged values at 1 s interval, corresponding to an along-track ground spacing of 370 m and 7.4 km, respectively. Four range values are calculated by four different tracking algorithms. Reference ellipsoid is WGS 84.

In this study, we used data from cycles 10 to 31, corresponding to a period from November 2002 to October 2004. The area of study is cross-cut by tracks 35, 78, 121, 407, 450, 493, 536, 579, 622, 908, 951 and 994.

River water stage from altimetry data selection

Over continents, radar echoes are affected by topography, vegetation, ice and snow cover. Indeed, a mountainous topography may cause the altimeter to lock off and it may take some time before it locks on again. In this case and with narrow rivers the instrument may fail to deliver reliable measurements. Also, the instrument may remain locked on water while the satellite is well ahead of the water body, since the reflected signal on water has more power than the reflected signal on land. This may cause a geometric error likely to reach several meters in some regions (Frappart et al., 2006).

As a result, the waveform (i.e., the power distribution over time of the radar echo) may not have the simple broad-peaked shape typical of ocean surfaces, but can be complex and multi-peaked (Berry, 2003; Birkett, 1998). The existing T/P and ENVISAT ocean retracking algorithms, the only one for T/P and one of four (OCEAN, ICE1, ICE2, SEAICE) for ENVISAT, are not designed to process these signals. This affects the precision in the determination of the altimetric height. Frappart et al. (2006) have shown that the tracker ICE1 was best suited to retrieve the ellipsoid height of continental water bodies.

To minimise potential contamination of the T/P and ENVISAT signal by land reflection, while securing an adequate number of altimeter measurements on water, we performed a geographical selection of data. We used JERS mosaic images of dry season from September to December 1995 and wet seasons from March to April 1996. Based on this mosaic, the most appropriate satellite tracks–river intersections could be selected with a high spatial resolution. Fig. 2 shows an example of data selected to define the so-called virtual stations.

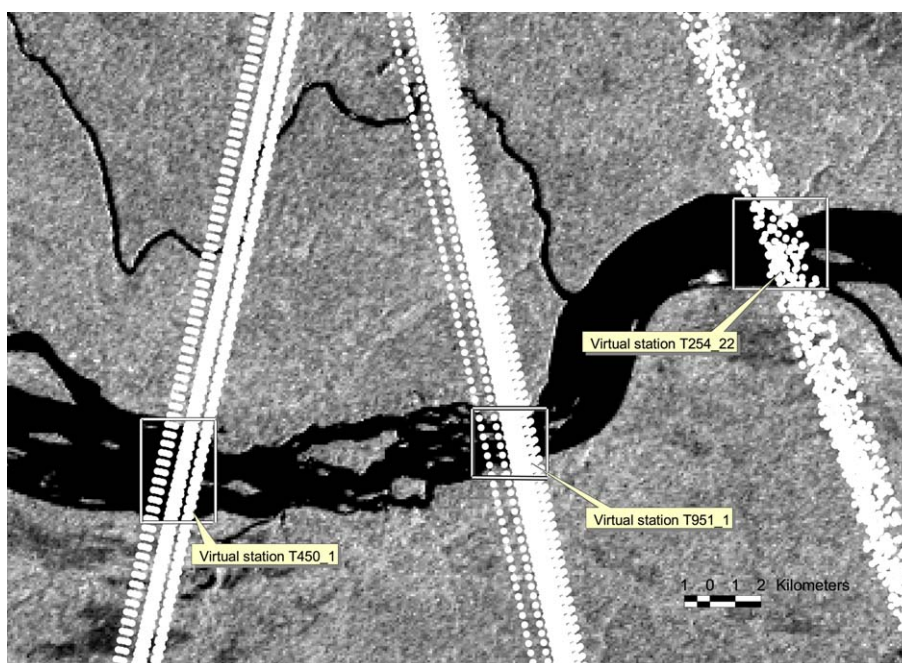


Figure 2 Virtual stations. Virtual stations selection data based on JERS image ENVISAT and T/P level measurements. The zone showed is located between Curicuriari and Serrinha in situ stations in dry season.

The width of the upper Negro River changes seasonally from 1 to 3 km in the main channel and over 8 km in floodplains depending on the phase of the hydrological regime and the geographic position. To arrive at consistent measurements in various phases of the water regime, we selected only those parts of the T/P and ENVISAT ground tracks that cover the main channel of the river system (Fig. 2). This stringent selection relied on the 1/10 s level measurements for T/P and 1/20 s for ENVISAT.

Despite the careful data selection as described above, altimetric water levels constitute data sets with numerous outliers. Frappart et al. (2006) have shown that the median of measurements for each pass is a better estimate of the water stage than the mean. This strategy has been followed in this study. Finally, unrealistic median values were last eliminated by visual comparison between water level and discharge time series for a given virtual station.

Modelled discharge data at virtual stations

Discharges at virtual stations were estimated using ProGUM, a M–C flow routing model with diffusion-cum-dynamic wave propagation assumption and in situ discharges (Leon et al., submitted for publication).

Flow routing models are normally used to estimate discharges in a section of the channel from a known hydrograph located at the upstream end (inflow hydrograph) and the physical characteristics of the reach.

In the M–C flow routing model (Cunge, 1969), that is an improvement of the classical Muskingum model, the well-known routing parameters X and K are derived from measured hydraulic data, especially, the rating curve, channel slope, channel width, wave velocity, reach length and flow discharge data (Ponce et al., 1996). M–C method avoids the calibration step required in the Muskingum method. In addition, the representation of diffusive waves can be imple-

mented when lateral flows are considered in the M–C algorithm (Ponce, 1986). Although M–C addresses only channel flows, considering lateral flows that can be positive or negative allows dealing globally with floodplain temporary storage and outflow, which are included into the lateral flows along with the localized rain input, and groundwater in- and outflows.

Leon et al. (submitted for publication) have developed, tested and validated the ProGUM model over the upper Negro River mainstream. The primary aim of that study was to estimate the discharges at different virtual stations of interest in the Negro River main stream. Discharges at virtual stations shown in Fig. 2 were estimated using in situ measurements from local stations. ProGUM model is extensively described in Leon et al. (submitted for publication). The model has supported discharge estimates with an error less than 10%, relative to measured discharges.

Rating curve and water depth estimation

Stage–discharge relationship or rating curve for gaging stations is developed using a set of discharge measurements and corresponding water level.

The relationship between stage and discharge is governed by a unique set or a combination of physical elements occurring downstream from the station, named controls. As outlined by Rantz et al. (1982), these controls may be classified into two groups, section control and channel control. Section control occurs when the geometry of a single cross-section located a short distance downstream from the gage is such that it constricts the channel, or when a downward break in bed slope occurs at the cross-section. Channel control occurs when the geometry and roughness of a long reach of channel downstream from the gaging station are the elements that govern the relationship between stage

and discharge. The length of reach that effectively governs the stage–discharge relation depends on the stream gradient, the lower the stream gradient, the longer the reach of channel control, and with respect to discharge, the larger the discharge, the longer the reach of channel control.

In natural river systems, a complete control governing the stage–discharge relationship throughout the entire range of stage experienced at the gaging station hardly ever exists. More commonly, the stage–discharge relationship for the gaging station results from a compound control or partial controls acting together.

Finally, at some gaging stations it may be difficult to retrieve a single equation describing the water stage–discharge relationship over the entire range of water stages experienced in the reach. A common approach is to build the stage–discharge relationship with the help of several segments only valid for a given range of stages.

In addition, some gaging stations may be influenced by variable backwater effects. These effects are normally caused by changes at downstream cross-sections. For example, the stations located a short distance upstream from a confluence in a flat region. The stage at the gaging station then depends on the stage at the confluence. In such a location, and under uniformly progressive wave flood conditions, a loop rating may be produced at the gaging station (Rantz et al., 1982): for a given stage, the discharge is greater when the stream is rising rather than falling. For these gaging stations, the rating requires the use of a slope, as well as stage, in relation with discharge.

These loop ratings have not been evidenced in any in situ stations used, and thus, most virtual stations located between these in situ stations are not likely to present loop rating. On the other hand, compound control of the gaging stations is likely to occur in some of the stations as is a common feature in natural river systems.

Rating curve

In order to model the stage–discharge relationship by a simple mathematical function, the Manning equation can be expressed as a power law, based on the continuity equation. Indeed, this equation can be modified to express the discharge of a channel control as follows:

$$Q = \frac{1}{n} AR^{2/3} S^{1/2}, \quad (1)$$

where Q is the discharge, n the roughness coefficient, A the cross-sectional area, R the hydraulic radius and S the friction slope.

In a natural channel of irregular shape it is possible to assume that at the higher stages the roughness coefficient is a constant and that the friction slope tends to become constant (Chow et al., 1988). Approximating $A = D \cdot W$ (where D is the average depth and W the width of the cross-section), and expressing $S^{1/2}/n$ as a constant a , we get:

$$Q \approx aDWR^{2/3}. \quad (2)$$

If the hydraulic radius is considered equal to D , and W is considered a constant, the equation becomes (Rantz et al., 1982):

$$Q \approx aD^{1.67} \approx a(H - z)^{1.67}. \quad (3)$$

In which $(H - z)$ stands for the water depth of the channel control, H the water stage level of the water surface and z the base of a rectangular-shaped section or the stage height of effective zero flow for a channel control or a section control of irregular shape. The gage level of effective zero flow is practically never reached but is actually a mathematical constant that is considered as a stage level to preserve the concept of a logarithmically linear head–discharge relationship.

In Eq. (3), Rantz et al. (1982) show that unless the stream is exceptionally wide, R is significantly smaller than D . This reduces the exponent in the equation although it may be offset by an increase of S or W with discharge. Changes in roughness with stage will also impact the exponent value. These factors allow us to express the discharge as follows:

$$Q_t = a(H - z)_t^b. \quad (4)$$

In which Q_t is the discharge and $(H - z)_t$ stands for the water depth of the control section at time t . Typically, a and b coefficients are specific to a channel cross-section. They can be related to the physical characteristics of the river. a is a scaling factor that encompasses the section width, the local bottom slope and Manning coefficient. b includes the geometry of the river banks, in particular the departure from vertical banks and generally an indicator of the type of control acting on the stage–discharge relation. A value of b less than 2 indicates a channel control and greater than 2 a section control (Rantz et al., 1982).

However, the water level data measured from space by radar altimeter refer to the ellipsoid of reference, in our case the WGS84 ellipsoid, and not to the bed of the channel. Thus, H in Eq. (4) is the water level given by the altimeter radar and z the elevation from the ellipsoid to the effective zero flow at time t . A rating equation such as Eq. (4) is developed for a particular river channel or cross-section and would not be expected to be applicable to any other river location. This is because the change in depth is used as an index corresponding to a change in width and velocity, and is specific to the channel characteristics of the reach being measured (Bjerklie et al., 2003).

Taking Q and h as known measured values, one has to arrive at the value of z that allows the water depth to be estimated from the zero flow of the channel at time t and the corresponding a and b coefficients. Rantz et al. (1982) rely on successive approximations to determine the effective zero flow based on the logarithmic rating-curve representation. However, for discharges in excess of 1000 m³/s, this methodology fails to estimate the value z that preserves the concept of a logarithmically linear stage–discharge relationship.

To determine the effective zero flow for any range of discharges, a methodology has been developed, consisting in the minimization of root mean square error (RMSE) between the modeled or measured discharge and the rated discharge. The RMSE can be expressed as follows:

$$\text{RMSE} = \sqrt{\frac{\sum (Q_{\text{mes}} - Q_{\text{calc}})^2}{n}}, \quad (5)$$

where Q_{mes} is the measured flow in the gauge case or the modeled discharge in the virtual gauge case, Q_{calc} is the rated flow and n the number of measurements considered.

Power law turns to a linear relationship in the logarithmic domain. Then, for a given z , the a and b coefficients are estimated by a linear regression through the $(\ln(Q), \ln(H - z))$ set. Exploring the range of possible values of z allows the function $RMSE(z) = f(z)$ to be built up. The entire range of possible z values has been explored by increments of 0.01 m. The value of z representing the effective zero flow altitude is such as

$$\frac{\partial f(z)}{\partial z} = 0. \quad (6)$$

The method was first applied at four gauge stations: Cucui, Sao Felipe, Curicuriari and Serrinha. The in situ dataset consists of water level, measured discharge and depth. It is worth noting that these depth measurements were all single points. They do not take into account depth variation across the section. Also, ADCP profiles have been collected at these stations during the field campaign in May 2005. Then, we searched for average depth at all virtual stations, comparing next to the ADCP profiles taken during the field campaign. Furthermore, a and b are evaluated for each site. As discussed above, these coefficients relate to section geometry. Their values determined through use of the power law fitting procedure are discussed in terms of river width and compared to widths for the dry and wet season measured on JERS mosaic images.

Slopes

Slope of river bed, as well as free surface slopes, have been calculated from interpolated altitude measurements, referenced to GCM02 geoid model (Tapley et al., 2005).

Results and discussion

Virtual stations over the Negro River main stream

Virtual stations are shown in Fig. 3. They correspond to the intersection of either T/P or ENVISAT crossings with Negro and Uaupes rivers.

Over the Negro River mainstream we defined 14 virtual stations. Three rely on T/P and 11 on ENVISAT. For the Uaupes River, one T/P and six ENVISAT virtual stations were also defined. The main characteristics of each station are summarized in Table 3.

Water stage and discharge estimations

Station T89_22 (Fig. 4b) is an example of water stages obtained from the processing of T/P data. Height variations are typical of the equatorial regime with a bimodal flood peak. On the contrary, the water level time series of T407_1 virtual station is an example of unimodal tropical regime (Fig. 4f). ENVISAT track 536 cross-cuts the Upper Rio Negro right at the Sao Felipe station. This gives us an opportunity to assess the quality of the time series of altimetry-derived water stages by straightforward comparison – i.e., without flow routing – with in situ readings. Both series of water in situ measured stage and altimetric height are displayed in Fig. 5. The RMS discrepancy between both – unbiased – series is 12 cm. This time series also highlights irregular features of flood events. It is worth pointing out that we decided to test our methodology on a more variable discharge regime than most of studies estimating discharges for Amazon basin (the main stem of the Amazon).

Discharges at the different T/P virtual stations were calculated by means of a M–C model described in Leon et al.

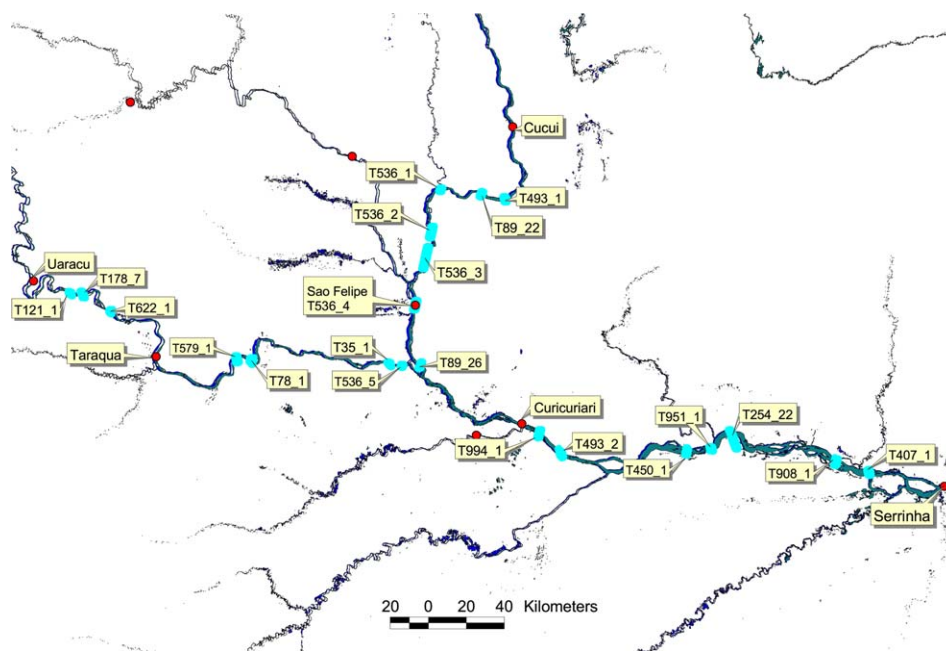


Figure 3 Virtual stations. Position of virtual stations between Cucui and Serrinha for the Negro River main stream and Uaracu et Curicuriari for the Uaupes River main stream.

Table 3 Principal characteristics of the virtual stations

Station	River	Latitude/longitude	Type of data	Dry/wet season cross-section width (km)	Discharge measured by ADCP in 05/2005 (m ³ /s)	Average water depth by ADCP in 05/2005 (m)	Upstream In situ station distance (km)
T493_1	Negro	0.87/−66.89	ENVISAT	1.72/2.23	7071	8.23	Cucui (47)
T89_22	Negro	0.91/−67.00	T/P	1.4/2.08	7071	8.40	Cucui (60)
T536_1	Negro	0.92/−67.19	ENVISAT	0.76/1.29	7623	10.18	Cucui (85)
T536_2	Negro	0.72/−67.23	ENVISAT	1.02/1.98	8582	11.43	Cucui (113)
T536_3	Negro	0.60/−67.26	ENVISAT	0.98/2.19	8647	9.32	Cucui (128)
T536_4	Negro	0.37/−67.31	ENVISAT	1.06/2.19	11,625	12.24	Sao Felipe (0)
T89_26	Negro	0.09/−67.29	T/P	0.8/0.84	12,524	11.95	Sao Felipe (33)
T994_1	Negro	−0.23/−66.73	ENVISAT	1.12/1.52	18,590	12.92	Curicuriari (10.6)
T493_2	Negro	−0.33/−66.62	ENVISAT	2.16/2.48	18,569	11.49	Curicuriari (26.5)
T450_1	Negro	−0.32/−66.03	ENVISAT	3.65/3.65	20,361	7.58	Curicuriari (100)
T951_1	Negro	−0.31/−65.91	ENVISAT	1.81/2.06	20,445	11.10	Curicuriari (114)
T254_22	Negro	−0.24/−65.81	T/P	2.72/7.70	21,841	11.48	Curicuriari (126)
T908_1	Negro	−0.37/−65.32	ENVISAT	2.91/2.91	22,388	12.44	Curicuriari (188)
T407_1	Negro	−0.41/−65.15	ENVISAT	2.44/2.44	23,460	11.78	Curicuriari (207)
T121_1	Uaupes	0.43/−68.94	ENVISAT	0.8/1.29	No data	No data	Uaracu (50.3)
T178_7	Uaupes	0.43/−68.89	T/P	0.98/0.98	No data	No data	Uaracu (57)
T622_1	Uaupes	0.35/−68.75	ENVISAT	1.06/1.69	No data	No data	Uaracu (80.4)
T579_1	Uaupes	0.12/−68.16	ENVISAT	1.21/2.64	4850	5.48	Taracua (60)
T78_1	Uaupes	0.11/−68.09	ENVISAT	1.42/1.42	4791	6.13	Taracua (69)
T35_1	Uaupes	0.11/−67.45	ENVISAT	0.89/1.41	5190	8.98	Taracua (160)
T536_5	Uaupes	0.09/−67.36	ENVISAT	1.02/1.34	5204	10.6	Taracua (168)

(submitted for publication) and the example of the discharge time series for Virtual Station T89_22 is shown in Fig. 4a. In these examples, discharge variations are clearly related to water levels variations. Despite the short measurements period for ENVISAT, the annual cycle of water levels is also clearly monitored, and discharge is correctly simulated by the model (Fig. 4a–d). Similar results have been obtained for all stations. Rating curves have been computed according to the methodology described above for all stations.

Rating curve and water depth estimation

Before estimating rating curves and water depth at each virtual station, we tested the method at four different in situ gauged stations: Cucui, Sao Felipe, Curicuriari and Serrinha. Similarly, we also validated the ADCP measurements at these stations in May 2005. The water stage given by the three methods, single-point measurement (GWD), average depth along the ADCP profile (MWD), and reference depth for the rating curve (EWD) are reported in Table 4. It is worth noting that all stages in Table 4 are related to the same discharge as measured by ADCP in May 2005. In Table 4, D1 stands for the difference between GWD and MWD. That D1 is not zero highlights the variability of in situ estimates for the reach depth, that can exceed 20%. For all stations, D2, that stands for the difference between GWD and MWD, is of the same order of magnitude as D1, and even smaller than D1 in three cases. The mean absolute difference between ADCP measured water depth and estimated zero flow water depth at these four stations is 68 cm, i.e., 6% of mean depth.

Table 5 lists the results of the computed rating curve at the 21 virtual stations taken into account in this study.

Reliability assessment of the rating curves parameters

Correlation coefficients for all rating curves are adequate for the ENVISAT virtual stations (Fig. 6). On the other hand, correlation coefficients found for the T/P virtual stations are below 0.8, thus pointing to a higher dispersion of the altimeter data (Fig. 6c and e). T/P data are known to be more scattered than ENVISAT ones over rivers (Frappart et al., 2006) since the T/P ranges are estimated only with an “ocean-like” tracker when the best performing tracker, e.g., ICE-1 (Bamber, 1994), could be selected among four for the ENVISAT ranges. As a result, the T/P altimetric data scattering turns the rating-curve difficult to adjust and this directly affects a and b coefficients and the reliability of estimated effective zero flow.

With the exception of station T89_26, all b values reported in Table 5 are below 2 indicating that the stage–discharge relationships are mostly channel-controlled at the studied virtual stations. As mentioned above, channel control is expected in a portion of the river where the geometry and roughness of a long reach of channel downstream from the gaging station are the elements that govern the relationship between stage and discharge.

Stations T89_26 yields a value of b greater than 2 indicating a stage to discharge relationship governed by a close downstream section. As reported in Fig. 3, this station is situated at Uaupes River and Negro River confluence. In this

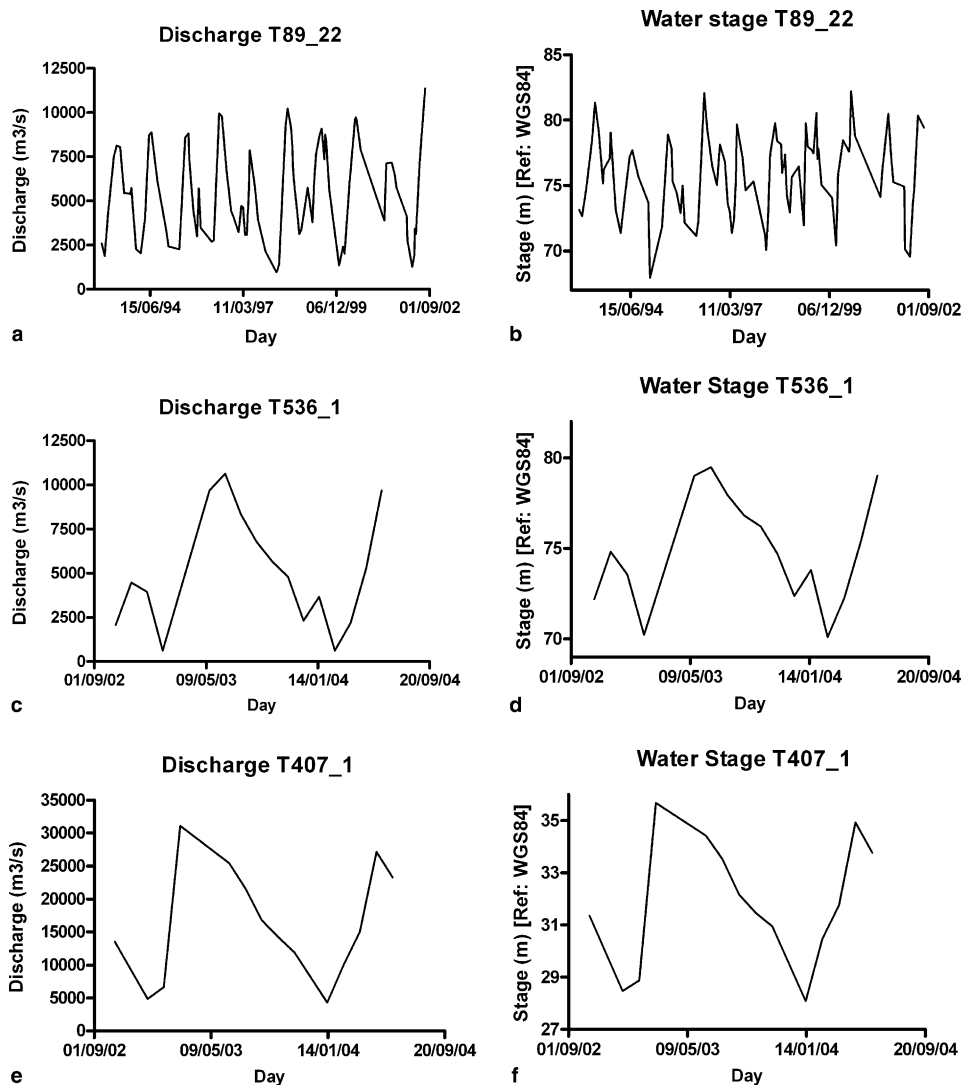


Figure 4 Discharge and water stage time series. Discharge and water stage time series of three virtual stations along the Negro River main stream.

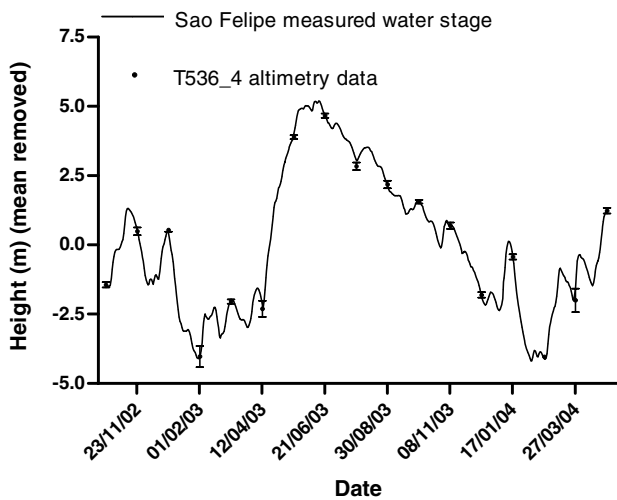


Figure 5 Time series of water stage at Sao Felipe. The thin continuous line stands for the daily in situ readings. ENVISAT heights (black dots) are reported as the median value at each pass (every 35 days) along with the standard deviation.

case, a section control might be expected. As discussed below, this b value greater than 2 can be also due to a downward break in bed slope at this section.

Based on Eq. (4) one can infer that values of coefficient a in Table 5 are strongly associated with three characteristics of the channel control: friction slope (S), Manning roughness coefficient (n) and mean width of cross-section (W). For most stations studied, the variations of a along the reaches are consistent with cross-section changes, slope changes and tributary inputs. Also, in station T254_22 a high value was found for a (1576). However, as reported in Table 3, this station features a 7 km width cross-section value during the rainy season. This characteristic, based on Eq. (4), leads to a high value for the coefficient a .

Reliability of the estimated zero flow depth compared with in situ depth measurements

Fig. 7 shows the evolution of RMS in discharge for some cross-sections when discharge–height pairs are fitted by a rating curve for successive values of reference depth z .

Table 4 Results of the method application at three gauged stations

Station	a	b	R^2	EWD (m)	GWD (m)	D1 (m)	D2 (m)	Difference between D1 and D2
Cucui	314.21	1.502	0.99	7.99	9.82	1.83	2.12	-0.29
Sao Felipe	179.08	1.86	0.97	11.53	11.75	0.22	-0.19	0.41
Curicuriari	33.13	2.495	0.96	13.6	11.03	2.57	0.73	1.84
Serrinha	105.73	2.308	0.94	10.83	11.78	0.95	0.77	0.19

GWD, gauged water depth at in situ station for the same discharge measured by the ADCP in 05/2005; EWD, estimated water depth by the rating curve for the same discharge measured by ADCP; D1, difference between GWD and EWD; D2, difference between GWD and MWD.

Table 5 Results of the rating-curve and water depth estimations at virtual stations

Station	a	b	z (m)	R^2	n	Average estimated water depth	EWD (m)	Difference between MWD and EWD (m)	σ_d (m)
T493_1	594.08	1.26	70.04	0.98	17	4.68	7.26	0.97	1.38
T89_22	339.83	1.25	67	0.66	86	8.85	8.28	0.12	1.48
T536_1	412.92	1.35	68.80	0.99	16	6.07	8.66	1.52	3.48
T536_2	105.21	1.79	65	0.90	19	8.25	11.74	-0.3	3.00
T536_3	206.56	1.63	66.34	0.98	18	6.85	10.05	-0.72	1.61
T536_4	179.08	1.86	65.29	0.97	18	8.38	10.95	1.30	4.1
T89_26	115.64	2.01	59.5	0.79	98	9.64	9.01	2.94	7.04
T994_1	204.92	1.87	36.51	0.99	15	8.12	11.01	0.72	5.45
T493_2	257.14	1.79	35.90	0.98	15	8.04	10.80	-0.69	3.76
T450_1	383.90	1.76	31.83	0.99	15	7.32	9.54	-1.95	2.57
T951_1	422.10	1.73	30.29	0.99	15	6.93	9.42	1.68	8.3
T254_22	1576	1.001	25	0.76	94	10.23	11.87	-0.39	4.67
T908_1	490.52	1.71	25.29	0.98	18	7.21	8.82	-1.16	2.44
T407_1	553.80	1.67	24.67	0.99	15	7.01	9.37	-2.41	4.54
T121_1	529.41	1.35	89.79	0.97	14	3.88	—	No MWD data	—
T178_7	340.95	1.41	88.29	0.72	59	4.23	—	No MWD data	—
T622_1	768.88	1.25	89.79	0.96	13	2.33	—	No MWD data	—
T579_1	175.80	1.71	73.97	0.99	13	4.55	6.78	-1.28	2.69
T78_1	410.41	1.36	74.11	0.97	14	4.72	6.092	0.04	3.26
T35_1	298.13	1.26	66.17	0.95	16	6.25	9.69	-0.71	3.94
T536_5	121.58	1.55	63.92	0.95	16	7.71	11.28	-0.68	3.45

GWD, gauged water depth at in situ station for the same discharge measured by the ADCP in 05/2005; EWD, estimated water depth by the rating curve for the same discharge measured by ADCP; MWD, measured average water depth by ADCP under each altimetric track in 05/2005; a , b , coefficients of the rating curve (Eq. (4)); z , estimated zero effective flow stage from the ellipsoid WGS84 by RMSE minimization method; R^2 , correlation coefficient of the rating curve; n , number of points in the rating curve; σ_d , standard deviation of the depth along the ADCP profile.

The minimum in RMS is always unique and well-defined. By comparing the results between estimated water depth and measured water depth in Table 5 we obtain an absolute mean difference of 1.2 m for all stations in Negro River and 0.67 m for those located on the Uaupes River. The method proposed seems rather robust and reliable, given the good agreement between measured and estimated depths.

ADCP cross-section profiles for each virtual station together with different estimates of mean water depth are shown in Figs. 8–10. Station T89_22 is not shown because only partial ADCP profile was available.

The profiles located between the Cucui and Sao Felipe stations (T493_1 and T536_1), upstream from the Negro and Uaupes rivers confluence are given in Fig. 8. Except

for station T536_1, it can be seen that the bottom irregularity of these sections is reduced and the depth can be reasonably approximated by some equivalent average value. In particular, a 380 m long island is evidenced along the section of the T493_1 virtual station (Fig. 8a). ADCP profiles collected from the confluence to Serrinha station (Fig. 9) differ substantially from the upstream ones. These profiles are very irregular and depth varies largely within each cross-section, especially for T89_26, T994_1, T450_1 and T951_1 stations. There, the characterization of the cross-section depth by a single value is less relevant. This finding is quantified at first-order by parameter σ_d reported in Table 5 which stands for depth variability along the ADCP profile. Indeed, variability of ± 7 m in MWD at T89_26 station for an average depth of 11.95 m or ± 8.3 m at T951_1 station for

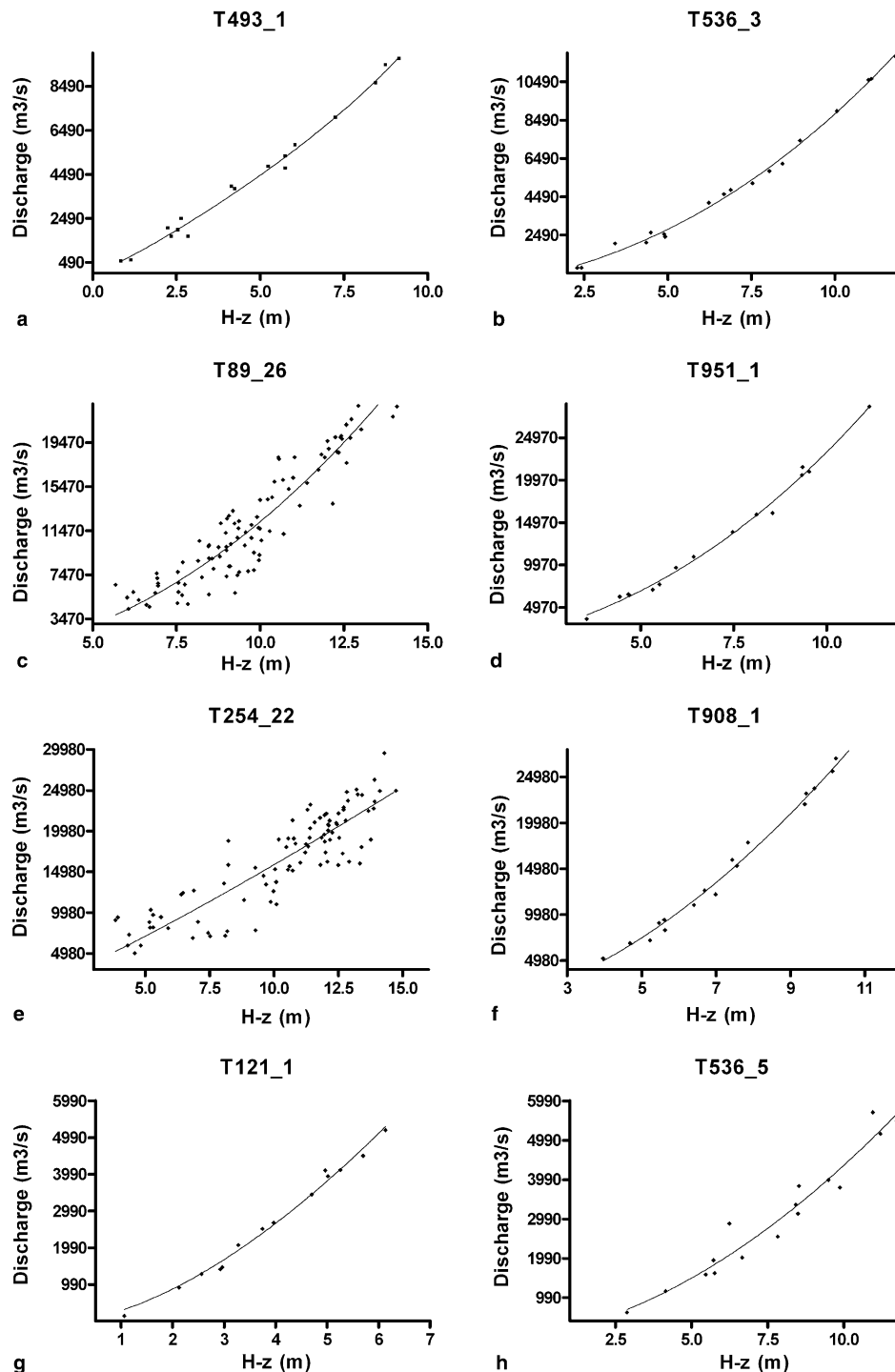


Figure 6 Estimated rating-curves. Example of estimated rating-curves for some virtual stations.

9.41 m average depth confirms the irregularity of the bottom shape and how difficult it is to measure a reliable equivalent water depth. The significant differences (>1 m) between EWD and MWD at these sections can be related to this fact or to the quality of the altimeter data. Indeed, these stations are located in areas where satellite measurements can be contaminated by the topography or physical characteristics of the river channel such as meanders, island systems and major confluences. More spatial data are re-

quired to reinforce and validate the rating-curves of these virtual stations. However, it can also be assumed that a mean depth measured from ADCP could be in these cases less reliable than the estimation of effective zero flow value. For the time being, it can only be stated that discrepancies are higher in the event of an irregular profile.

At the downstream end of the reach, between T254_22 and T407 stations (Fig. 9b–d), the width section changes by 1.5 km between high and low waters. This significant

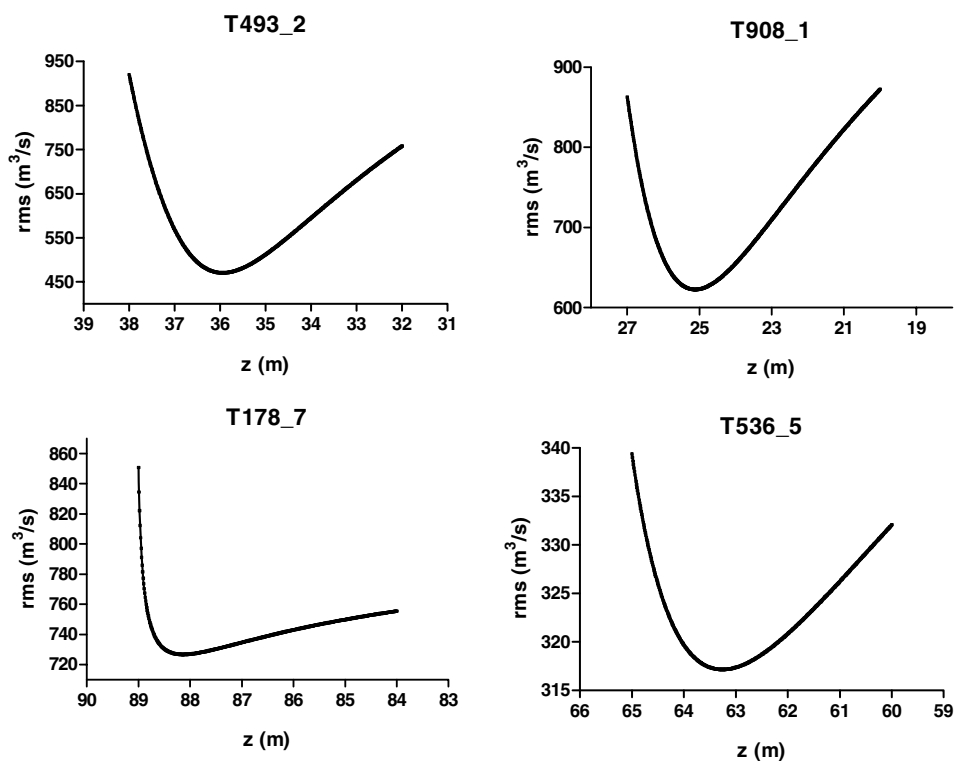


Figure 7 RMS evolution. Evolution of the RMS in discharge when the discharge–height pairs are fitted by a rating curve for successive values of the reference depth z .

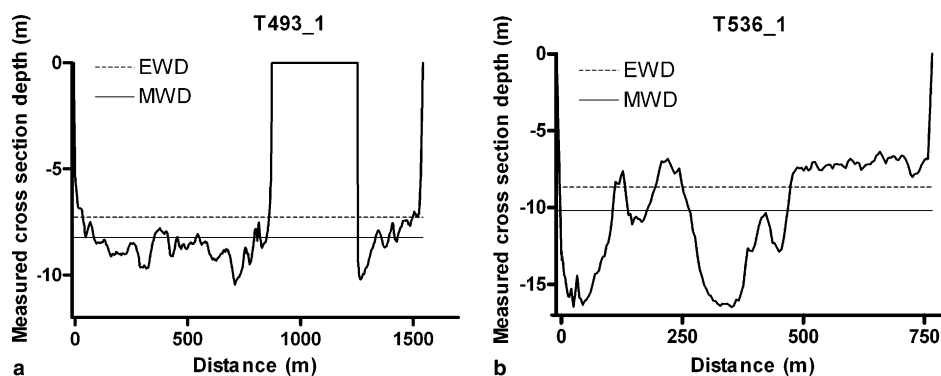


Figure 8 ADCP profiles from Cucui to Sao Felipe station (following down the Rio Negro). Measured profiles by ADCP in May 2005 for the virtual stations located between Cucui and Sao Felipe.

width variation could also account for the value of a found in station T254_22.

Lastly, some cross-section profiles are given in Fig. 10 for the Uaupes River. σ_d ranges from ± 2.7 m at T579_1 station and ± 4 m at T35_1 station, for an average water depth of ~ 7 m. Again, irregularity at the cross-sections detrimentally affects the estimate of typical water depth.

As shown in Table 5, for all stations with ADCP profile EWD values were found that do not depart from MWD by more than σ_d . Thus, it can be concluded that the method presented in this study provides reliable estimates EWD of the equivalent zero flow from remote discharges and altimeter data.

Bottom slope compared with free surface slope during low and high water stages

The average bottom slope of the upper Negro River basin can be calculated on the basis of the zero effective flow estimations presented in Table 5 (Fig. 11). For the reach from T493_1 station to T536_4 station, upstream from the confluence with Uaracu River, we computed a bed slope of $4.56 \times 10^{-5} \text{ m m}^{-1}$. From T89_26 station to 994_1 station, downstream from the confluence, the bed channel of the river shows a major increase in bottom slope, namely $2.4 \times 10^{-4} \text{ m m}^{-1}$. This section of the river is so-called *Sao Gabriel da*

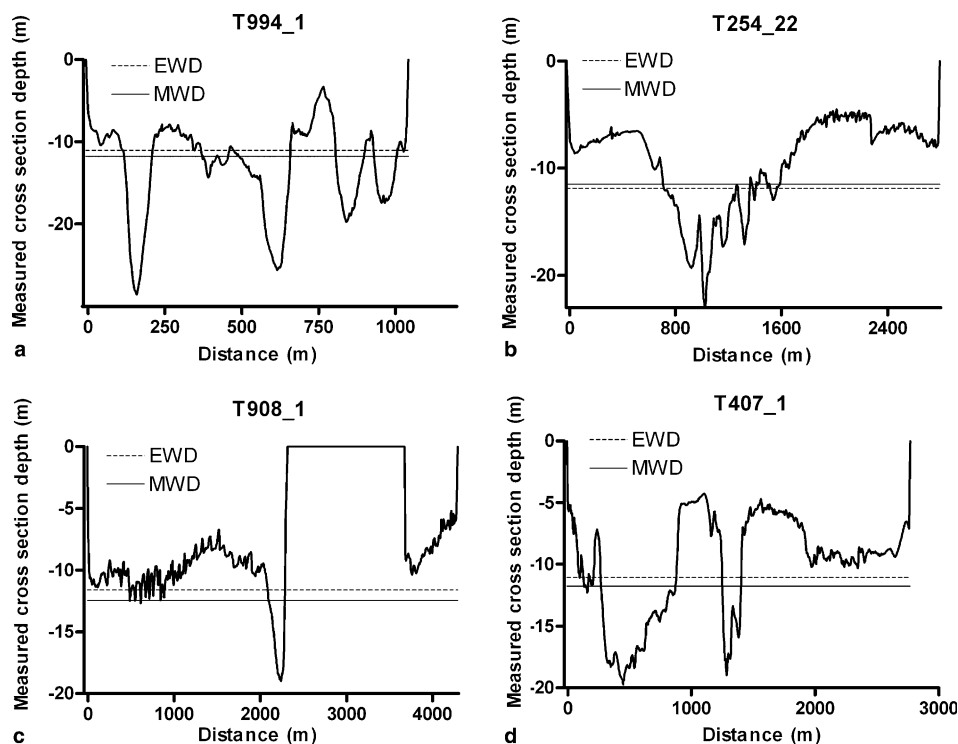


Figure 9 ADCP depth profiles at the virtual stations (following the Rio Negro, from Sao Felipe to Serrinha). Profiles collected in May 2005.

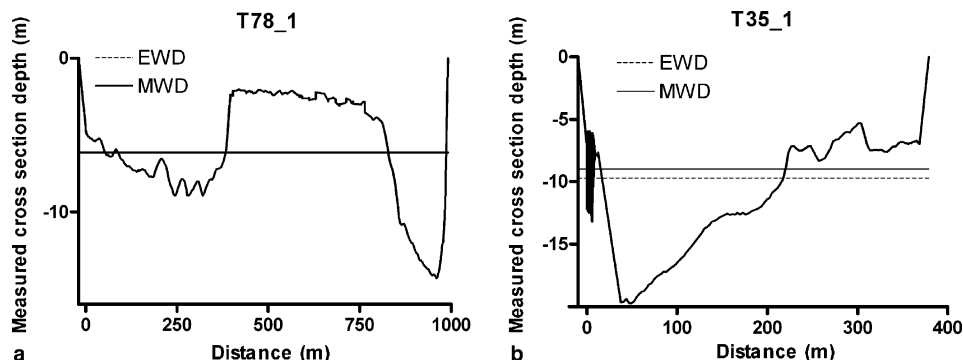


Figure 10 Uaupes River profiles. Measured profiles by ADCP in May 2005 for the virtual stations located at Uaupes River main stream.

Cachoeira (Sao Gabriel Waterfall). With a denser network of stations due to the addition of virtual stations, the method even allows us to track the major changes in bed slope. Finally, a bed slope of $6.86 \times 10^{-5} \text{ m m}^{-1}$ is found for the most downstream reach of the upper Negro River main stream.

Similarly, the Uaupes River bed slope was estimated from stations T121_1 to T536_5 (Fig. 12). An average slope of $1.02 \times 10^{-4} \text{ m m}^{-1}$ was calculated for this reach. A major change in slope was found between T622_1 and T579_1 virtual stations.

These results can be compared with the free water surface slope calculated from ENVISAT altimetry data. Fig. 13 shows the profile of free water slope in dry season, rain season and the bottom slope of the upper Negro River between T536_1 and T407_1 ENVISAT virtual stations. A very good agreement is found between the free surface slope and

the bottom slope, providing an external validation of this method for water depth estimation at virtual stations. The agreement between the free surface and bed slopes also validates the assumption we made of kinematic slope.

Estimation of Manning roughness coefficient

Combining the Manning equation (1) and rate to discharge relationship equation (4), the Manning roughness coefficient (n) can be derived from known values of a , S and W . Mean bottom slope values were used from T493_1 to T536_4 virtual stations, T89_26 to T994_1, 493_2 to T254_22, and T908_1 and T407_1 for the Negro River main stream. Width (W) values were estimated using JERS images acquired during the dry and rainy seasons. Thus, the n values were estimated at the different reaches with the same physical

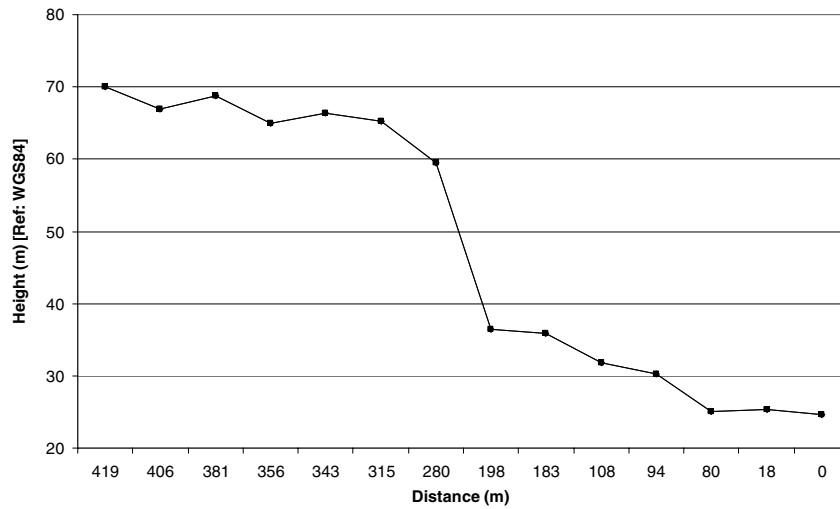


Figure 11 Negro River bed slope. Upper Negro River bottom slope profile.

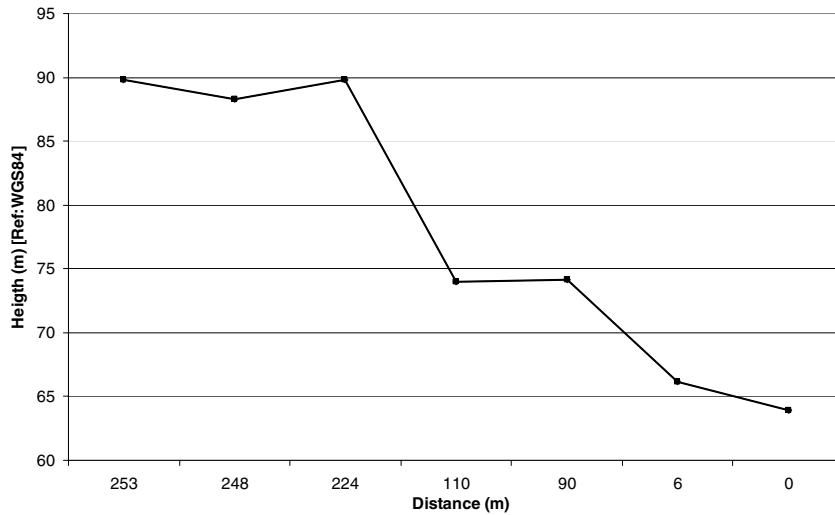


Figure 12 Uaupes River bed slope. Uaupes River bottom slope profile.

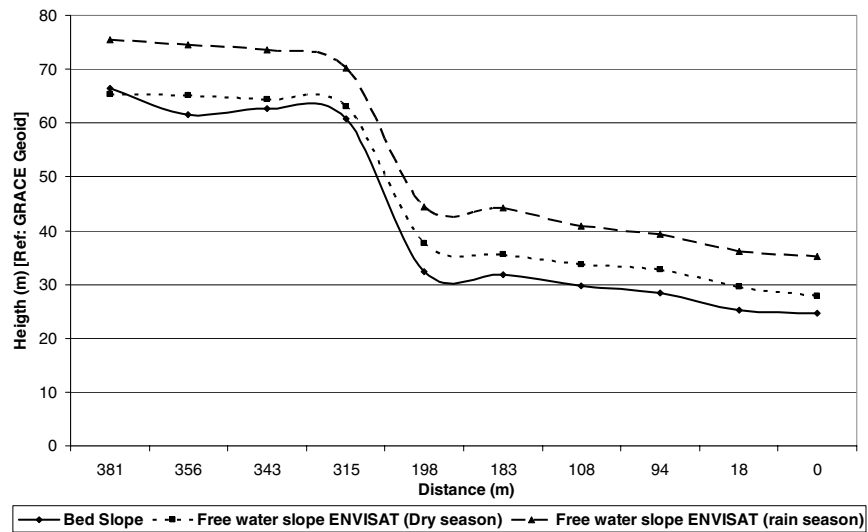


Figure 13 Negro River free water slope and bed slope. Upper Negro River free water slope calculated from ENVISAT altimetry data in dry and rainy season; and estimated bed slope.

Table 6 Manning roughness coefficient along the Negro and Uaupes Rivers

Reach	Reach number	<i>n</i> (dry season)	<i>n</i> (rain season)
T493_1–T536_4	1	0.04	0.076
T89_26–T994_1	2	0.093	0.11
T493_2–T254_22	3	0.037	0.04
T908_1–T407_1	4	0.032	0.032
T121_1–T536_5	5	0.036	0.054

characteristics considering changes in slope, and the presence of the island systems. For the Uaupes River, we only considered one average bottom slope from T121_1 to 536_5. Table 6 summarizes the resulting Manning coefficient values found for these reaches during the dry and rain seasons.

Values of roughness coefficient reported in Table 6 are consistent with values suggested by Chow (1959). For major flows (width >30 m) with an irregular section, Chow (1959) suggests that Manning's coefficient ranges from 0.035 to 0.1. The highest values correspond to irregular natural channels with significant variations in cross-section, major obstructions, and the presence of vegetation, meanders and islands. Values reported in Table 6 indicate that the Negro River behaves as channels with irregular and roughness section in reaches 1, 3 and 4 with an *n* mean value between dry and rainy season of 0.036 and of 0.049, respectively. Similarly, the Uaupes River (reach 5) has a mean *n* value of 0.045 suggesting physical characteristics similar to those of the Negro River. On the other hand, higher values of *n* are obtained in reach 2. As discussed above, the stations considered are located in a river portion of complex geometry directly impacting hydrodynamics. As indicated in Chow (1959), a strong slope, meanders and islands lead to higher values of *n*.

Conclusions

This work highlights a very promising application of the spatial altimetry over inland waters, especially over the great fluvial basins such as the Amazon basin, but in areas within this basin where both geometry and discharge are very irregular (upstream reaches of Rio Negro sub-basin). The estimation of the stage–discharge relationship at virtual stations with a high accuracy from calculated remote discharges and filtered altimeter data are a new field in the spatial hydrology. We estimated the rating-curves for 21 virtual stations at the upper Negro River basin: 14 along the Negro River main stream between Cucui and Serrinha gauged stations and 7 along the Uaupes River from Uaracu station to the confluence with Negro mainstream (Fig. 3).

The RMSE minimization method presented in this paper has allowed us to estimate the zero effective flow and consequently the water depth of these 21 cross-sections with an average difference less than 1.1 m between measured water depth and estimated water depth. It can be stated that the preliminary results and the performance of the method are reliable. This is supported by EWD values lying within one standard deviation from the MWD. Using the rat-

ing curves obtained at the successive virtual stations allowed us to estimate consistent Manning roughness coefficients have been estimated and we determined the flow propagation conditions (either channel or section controlled). Our method allows us to extract bottom elevation, bottom and free surface slopes and roughness coefficients from a combination of altimeter and remote discharge data. These quantities are highly valuable for understanding rivers and hydrodynamic modelling. The methodology developed should support future work on the Amazon Basin where hydrodynamic modelling had always been prevented by the lack of in situ data.

Acknowledgements

This study was funded by the CASH project from the "Réseau Terre & Espace" of the French Ministry of Research and Technology (MR decision No. 04 T 131), and by the ECCO PNRH MESBAM project. We are very grateful to the reviewers of this work, for their helpful remarks. We address special thanks to Gerard Cochonneau, who is in charge of the Hybam in situ database and is always more than helpful by sharing his great experience in discharge data processing and stage to discharge relationship computing. Finally, our thanks are addressed to Jean Loup Guyot for the passionate discussions about the measurement of river bed from space.

References

- AVISO User Handbook, 1996. Merged TOPEX/Poseidon Products (GDR-Ms), AVI-NT-02-101-CN, Edition 3.0.
- Bamber, J.L., 1994. Ice sheet altimeter processing scheme. *Int. J. Remote Sensing* 15 (4), 925–938.
- Barrett, E., 1998. Satellite remote sensing in hydrometry. In: Herschey (Ed.), *Hydrometry: Principles and Practices*, second ed. Wiley, Chichester, pp. 199–224.
- Berry, P.A., 2003. Global river and lake monitoring from multimission altimetry: capability and potential. In: *The Abstracts of the Workshop Hydrology from Space*, 29 September–1 October 2003, Toulouse, France.
- Birkett, C.M., 1995. The contribution of Topex/Poseidon to the global monitoring of climatically sensitive lakes. *J. Geophys. Res.* 100 (C12), 25179–25204.
- Birkett, C., 1998. The contribution of TOPEX NASA radar altimeter to the global monitoring of large rivers and wetlands. *Water Resour. Res.* 34, 1223–1239.
- Birkett, C.M., Mertes, L.A., Dunne, T., Costa, M., Jasinski, J., 2002. Altimetric remote sensing of the Amazon: application of satellite radar altimetry. *J. Geophys. Res.* 107 (D20), 8059. doi:10.1029/2001JD000609.
- Birkhead, A., James, C., 1998. Synthesis of rating curves from local stage and remote discharge monitoring using nonlinear Muskingum routing. *J. Hydrol.* 205, 52–65.
- Bjerklie, D.M., Dingman, S.L., Vorosmarty, C.J., Bolster, C.H., Congalton, R.G., 2003. Evaluating the potential for measuring river discharge from space. *J. Hydrol.* 278 (14), 17–38.
- Boroughs, C., Zagona, E., 2002. Daily flow routing with the Muskingum–Cunge method in the Paecos River Riverware Model. In: *Proceedings of the Second Federal Interagency Hydrologic Modeling Conference*, Las Vegas, NV, July.
- Cazenave, A., Bonnefond, P., DoMinh, K., 1997. Caspian Sea level from Topex/Poseidon altimetry: level now falling. *Geophys. Res. Lett.* 24, 881–884.

- Chow, V.T., 1959. *Open Channel Hydraulics*. McGraw-Hill, New York.
- Chow, V.T., Maidment, D., Mays, L., 1988. *Applied Hydrology*. McGraw-Hill, New York.
- Coe, M., Costa, M., Botta, A., Birkett, C.M., 2002. Long-term simulations of discharge and floods in the Amazon Basin. *Geophys. Res.* 107 (D20). doi:10.1029/2001JD000740.
- Cunge, J.A., 1969. On the subject of a flood propagation computation method (Muskingum method). *Hydraul. Res.* 7 (2), 205–230.
- Dubroeuq, D., Volkoff, B., 1998. From oxisols to spodosols and histosols: evolution of the soil mantles in the Negro River basin (Amazonia). *Catena* 32, 245–280.
- Frappart, F., Calmant, S., Cauhope, M., Seyler, F., Cazenave, A., 2006. Preliminary results of ENVISAT RA-2-derived water levels validation over the Amazon Basin. *Remote Sens. Environ.* 100 (2), 252–264.
- Guyot, J.L., 1993. Hydrogéochimie des fleuves de l'Amazonie Bolivienne. In: *Géologie, Géochimie*, Université Bordeaux I, Bordeaux, p. 261 (in French).
- Jasinski, M.J., Birkett, C.M., Chinn, S., Costa, M.H., 2001. In: Abstract, NASA/NOAA GAPP and Hydrology Principal Investigators Meeting, April 30–May, Potomac, MD.
- Johnson, D., Miller, A., 1997. A spatially distributed hydrologic model utilizing raster data structures. *Comput. Geosci.* 23 (3), 267–272.
- Leon, J.G., Bonnet, M.P., Cauhope, M., Calmant, S., Seyler, F., submitted for publication. Distributed water flow estimates of the upper Negro River using a Muskingum–Cunge routing model based on altimetric spatial data. *J. Hydrol.*
- Merkel, W., 1999. Muskingum–Cunge Flood Routing Procedure in NRCS Hydrologic Models. USDA NRCS, National Water and Climate Center, Beltsville.
- Ponce, V.M., 1986. Diffusion wave modelling of catchment dynamics. *J. Hydraul. Div., ASCE* 112 (8), 716–727.
- Ponce, V.M., Lohani, A., Scheyhing, C., 1996. Analytical verification of Muskingum–Cunge routing. *J. Hydrol.* 174, 235–241.
- Rantz, S.E. et al., 1982. *Measurement and computation of streamflow. Measurement of Stage and Discharge*, US Geological Survey Water Supply Paper, vol. 1, p. 284.
- Renellys, C., Perez, Dudley, B., Chelton, Robert, N. Miller, 2005. The effects of wind forcing and background mean currents on the latitudinal structure of equatorial Rossby waves. *J. Phys. Oceanogr.* 35 (5), 666–682.
- Richey, J., Mertes, A., Dunne, T., Victoria, R., Forsberg, B., Tancredi, A., Oliveira, E., 1989. Sources and routing of the Amazon River flood wave. *Global Biochem. Cycl.* 3 (3), 191–204.
- Soil Survey Staff, 1975. *Soil Taxonomy. Basic System of Soil Classification for Making and Interpreting Soil Surveys*. USDA, Washington, Agricultural Handbook 436, 754 pp.
- Soil Survey Staff, 1990. *Keys to Soil Taxonomy*. Agency for International Development. USDA Soil Management Support Services. Technical Monograph 19, fourth ed., Virginia Polytechnic Institute and State University.
- Tapley, B., Ries, J., Bettadpur, S., Chambers, D., Cheng, M., Condi, F., Gunter, B., Kang, Z., Nagel, P., Pastor, R., Pekker, T., Poole, S., Wang, F., 2005. GGM02 — An improved Earth gravity field model from GRACE. *J. Geodesy* 79 (8), 467–478.